

FastDOG: Fast Discrete Optimization on GPU

Ahmed Abbas Paul Swoboda

Max Planck Institute for Informatics, Saarland Informatics Campus

Abstract

We present a massively parallel Lagrange decomposition method for solving 0–1 integer linear programs occurring in structured prediction. We propose a new iterative update scheme for solving the Lagrangean dual and a perturbation technique for decoding primal solutions. For representing subproblems we follow [37] and use binary decision diagrams (BDDs). Our primal and dual algorithms require little synchronization between subproblems and optimization over BDDs needs only elementary operations without complicated control flow. This allows us to exploit the parallelism offered by GPUs for all components of our method. We present experimental results on combinatorial problems from MAP inference for Markov Random Fields, quadratic assignment and cell tracking for developmental biology. Our highly parallel GPU implementation improves upon the running times of the algorithms from [37] by up to an order of magnitude. In particular, we come close to or outperform some state-of-the-art specialized heuristics while being problem agnostic.

1. Introduction

Solving integer linear programs (ILP) efficiently on parallel computation devices is an open research question. Done properly it would enable more practical usage of many ILP problems from structured prediction in computer vision and machine learning. Currently, state-of-the-art generally applicable ILP solvers tend not to benefit much from parallelism [42]. In particular, linear program (LP) solvers for computing relaxations benefit modestly (interior point) or not at all (simplex) from multi-core architectures. In particular generally applicable solvers are not amenable for execution on GPUs. To our knowledge there exists no practical and general GPU-based optimization routine and only a few solvers for narrow problem classes have been made GPU-compatible e.g. [1, 45, 54, 61]. This, and the superlinear runtime complexity of general ILP solvers has hindered application of ILPs in large structured prediction problems, necessitating either restriction to at most medium problem sizes or difficult and time-consuming development of specialized

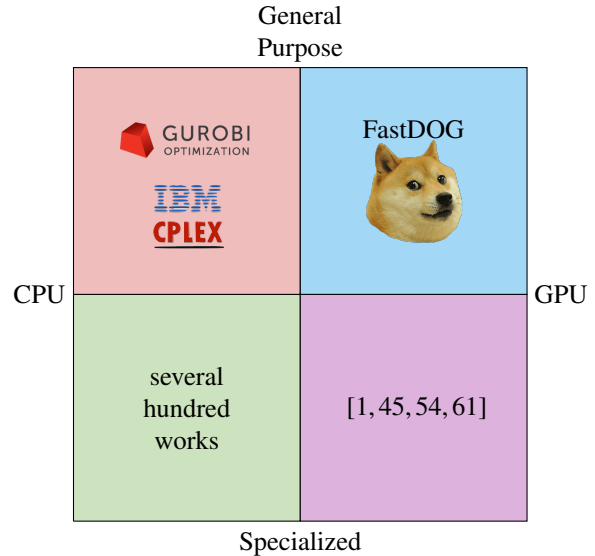


Figure 1. Qualitative comparison of ILP solvers for structured prediction. Our solver (FastDOG) is faster than Gurobi [20] and comparable to specialized CPU solvers, but outperformed by specialized GPU solvers. FastDOG is applicable to a diverse set of applications obviating the human effort for developing solvers for new problem classes.

solvers as observed for the special case of MAP-MRF [30].

We argue that work on speeding up general purpose ILP solvers has had only limited success so far due to complicated control flow and computation interdependencies. We pursue an overall different approach and do not base our work on the typically used components of ILP solvers. Our approach is designed from the outset to only use operations that offer sufficient parallelism for implementation on GPUs.

We argue that our approach sits on a sweet spot between general applicability and efficiency for problems in structured prediction as shown in Figure 1. Similar to general purpose ILP solvers [14, 20], there is little or no effort to adapt these problems for solving them with our approach. On the other hand we outperform general purpose ILP solvers in terms of execution speed for large problems from structured prediction and achieve runtimes comparable to hand-crafted specialized CPU solvers. We are only significantly

outperformed by specialized GPU solvers. However, development of fast specialized solvers especially on GPU is time-consuming and needs to be repeated for every new problem class.

Our work builds upon [37] in which the authors proposed a Lagrange decomposition into subproblems represented by binary decision diagrams (BDD). The authors proposed sequential algorithms as well as parallel extensions for solving the Lagrange decomposition. We improve upon their solver by proposing massively parallelizable GPU amenable routines for both dual optimization and primal rounding. This results in significant runtime improvements as compared to their approach. We will make our code available upon acceptance of the paper.¹

2. Related Work

General Purpose ILP Solvers & Parallelism The most efficient implementation of general purpose ILP solvers [14, 20] provided by commercial vendors typically benefit only moderately from parallelism. A recent survey is this direction is given in [42]. The main ways parallelism is utilized in ILP solvers are:

Multiple Independent Executions State-of-the-art solvers [14, 20] offer the option of running multiple algorithms (dual/primal simplex, interior point, different parameters) solving the same problem in parallel until one finds a solution. While easy to do and worthwhile for problems for which it is unknown which algorithms resp. parameter configurations are best, such a simple approach can deliver parallelization speedups only to a limited degree.

Parallel Branch-and-bound tree traversal While appealing on first glance, it has been observed [43] that the order in which a branch-and-bound tree is traversed is crucial due to exploitation of improved lower and upper bounds and generated cuts. Consequently, it seems hard to obtain significant parallelization speedups and many recent improvements rely on a sequential execution. A separate line of work [47] exploited GPU parallelism for domain propagation allowing to decrease the size of the branch-and-bound tree.

Parallel LP-Solver Interior point methods rely on computing a sequence of solutions of linear systems. This linear algebra can be parallelized for speeding up the optimization [17, 46]. However, for sparse problems sequential simplex solvers still outperform parallelized interior point methods. Also, a crossover step is needed to obtain a suitable basis for the simplex method for

reoptimizing for primal rounding and in branch-and-bound searches, limiting the speedup obtainable by this sequential bottleneck. The simplex method is less straightforward to parallelize. The work [25] reports a parallel implementation, however current state-of-the-art commercial solvers outperform it with sequentially executed implementations.

Machine Learning Methods Recently deep learning based methods have been proposed for choosing variables to branch on [15, 40] and for directly computing some easy to guess variables of a solution [40] or improving a given one [48]. While parallelism is not the goal of these works, the underlying deep networks are executed on GPUs and hence the overall computation heavy approach is fast and brings speedups. Still, these parallel components do not replace the sequential parts of the solution process but work in conjunction with them, limiting the overall speedup attainable.

A shortcoming of the above methods in the application to very large structured prediction problems in machine learning and computer vision is that they still do not scale well enough to solve problems with dozens of million variables in a few seconds.

Parallel Combinatorial Solvers For specialized combinatorial problem classes highly parallel algorithms for GPU have been developed. For Maximum-A-Posteriori inference in Markov Random Fields [45, 61] proposed a dual block coordinate ascent algorithm for sparse and [54] for dense graphs. For multicut a primal-dual algorithm has been proposed in [1]. Max-flow GPU implementations have been investigated in [56, 60]. While some parts of the above specialized algorithms can potentially be generalized, other key components cannot, limiting their applicability to new problem classes and requiring time-consuming design of algorithms whenever attempting to solve a different problem class.

Specialized CPU solvers There is a large literature of specialized CPU solvers for specific problem classes in structured prediction. For an overview of pursued algorithmic techniques for the special case of MRFs we refer to the overview article [30]. Most related to our approach are the so called dual block coordinate ascent (a.k.a. message passing) algorithms which optimize a Lagrange decomposition. Solvers have been developed for MRFs [16, 27, 28, 33, 34, 39, 44, 54, 55, 57, 58], graph matching [50, 51, 62], multicut [1, 36, 49], multiple object tracking [24] and cell tracking [21]. Most of the above algorithms require a sequential computation of update steps.

¹Code can be viewed at anonymous.4open.science/r/FADOP-4E2D

| | |
|-----------------|--|
| x_i | Optimization variable $i \in [n]$ |
| \mathcal{X}_j | Feasible set of constraint $j \in [m]$ |
| \mathcal{I}_j | Set of variables in constraint $j \in [m]$ |
| \mathcal{J}_i | Set of constraints containing variable $i \in [n]$ |
| m_{ij}^β | Min-marginal for variable i taking value β in subproblem $j \in [m]$ |
| λ_i^j | Lagrange multiplier for variable i in subproblem j |

Table 1. Notation of symbols used in our problem decomposition.

Optimization with Binary Decision Diagrams Our work builds upon [37]. The authors proposed a Lagrange decomposition of ILPs that can be optimized via a sequential dual block coordinate ascent method or a decomposition based approach that can utilize multiple CPU cores.

The works [4, 5, 38] similarly consider decompositions into multiple BDDs and solve the resulting problem with general purpose ILP solvers. The work [6] investigates optimization of Lagrange decompositions with multi-valued decision diagrams with subgradient methods. An extension for job sequencing was proposed in [23] and in [13] for routing problems. Hybrid solvers using mixed integer programming solvers were investigated in [18, 19, 52]. The works [2, 7, 8] consider stable set and max-cut and propose optimizing (i) a relaxation to get lower bounds [2] or (ii) a restriction to generate approximate solutions [7, 8].

In contrast to previous BDD-based optimization methods we propose a highly parallelizable and problem agnostic approach that is amenable to GPU computation.

3. Method

We first introduce the optimization problem and its Lagrange decomposition. Next we elaborate our parallel update scheme for optimizing the Lagrangean dual followed by our parallel primal rounding algorithm. For the problem decomposition and dualization we follow [37]. Our notation is summarized for reference in Table 1.

Definition 1 (Binary Program). Consider a linear objective $c \in \mathbb{R}^n$ and m variable subsets $\mathcal{I}_j \subset [n]$ of constraints with feasible set $\mathcal{X}_j \subset \{0, 1\}^{\mathcal{I}_j}$ for $j \in [m]$. The corresponding binary program is defined as

$$\min_{x \in \{0, 1\}^n} \langle c, x \rangle \quad \text{s.t.} \quad x_{\mathcal{I}_j} \in \mathcal{X}_j \quad \forall j \in [m], \quad (\text{BP})$$

where $x_{\mathcal{I}_j}$ is the restriction to variables in \mathcal{I}_j .

Example 1 (ILP). Consider the 0–1 integer linear program

$$\min c^\top x \quad \text{s.t.} \quad Ax \leq b, x \in \{0, 1\}^n. \quad (\text{ILP})$$

The system of linear constraints $Ax \leq b$ may be split into m blocks, each block representing a single (or multiple)

rows of the system. For instance, let $a_j^\top x \leq b_j$ denote the j -th row of $Ax \leq b$, then the problem can be written in the form (BP) by setting $\mathcal{I}_j = \{i \in [n] : a_{ji} \neq 0\}$ and $\mathcal{X}_j = \{x \in \{0, 1\}^{\mathcal{I}_j} : \sum_{i \in \mathcal{I}_j} a_{ji} x_i \leq b_j\}$.

3.1. Lagrangean Dual

While (BP) is NP-hard to solve, optimization over a single constraint is typically easier (but may still be NP-hard e.g. for Knapsack). Below we dualize the original problem using Lagrange decomposition similarly as in [37]. This allows us to solve the Lagrangean dual of the full problem (BP) by iteratively solving only the subproblems.

Definition 2 (Lagrangean dual problem). Define the set of subproblems that constrain variable x_i as $\mathcal{J}_i = \{j \in [m] \mid i \in \mathcal{I}_j\}$. Let the energy for subproblem $j \in [m]$ w.r.t. Lagrangean dual variables $\lambda^{j, \beta} \in \mathbb{R}^{\mathcal{I}_j}$ for $\beta \in \{0, 1\}$ be

$$E^j(\lambda^j) = \min_{x \in \mathcal{X}_j} x^\top \lambda^j. \quad (1)$$

Then the Lagrangean dual problem is defined as

$$\max_{\lambda} \sum_{j \in [m]} E^j(\lambda^j) \quad \text{s.t.} \quad \sum_{j \in \mathcal{J}_i} \lambda_i^j = c_i \quad \forall i \in [n]. \quad (\text{D})$$

If optima of the individual subproblems $E^j(\lambda^j)$ agree with each other then the consensus vector obtained from stitching together individual subproblem solutions solves the original problem (BP). In general, (D) is a lower bound on (BP). Formal derivation of (D) is done as in [37].

3.2. Min-Marginals

We use min-marginals in our optimization algorithms. These quantities allow us to derive Lagrange variable update steps that result in improvements of the dual lower bound (D). We also use min-marginals for primal rounding.

Definition 3 (Min-marginals [37]). For $i \in [n]$, $j \in \mathcal{J}_i$ and $\beta \in \{0, 1\}$ let

$$m_{ij}^\beta = \min_{x \in \mathcal{X}_j} x^\top \lambda^j \quad \text{s.t.} \quad x_i = \beta \quad (\text{MM})$$

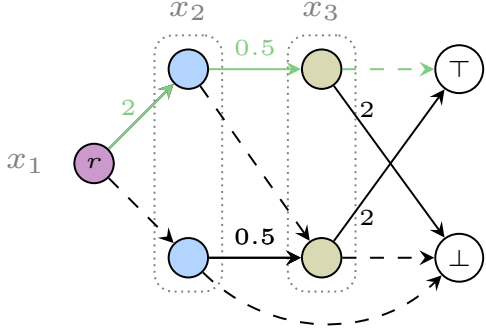
denote the *min-marginal* w.r.t. i, j and β .

The quantity $|m_{ij}^1 - m_{ij}^0|$ indicates by how much $E^j(\lambda^j)$ increases if x_i is fixed to 1 (if $m_{ij}^1 > m_{ij}^0$), respectively 0 (if $m_{ij}^1 < m_{ij}^0$). Thus, if $m_{ij}^1 > m_{ij}^0$ then assigning a 0 to variable i has a lower cost than assigning a 1 in the subproblem j .

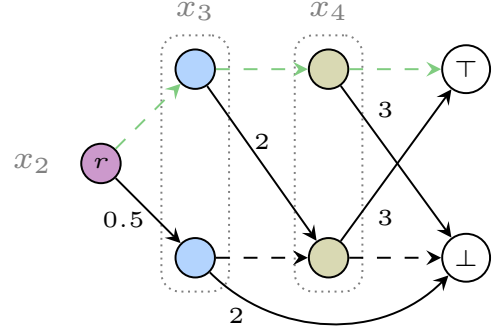
Min-marginals have been used in various ways to design dual block coordinate ascent algorithms [1, 3, 16, 21, 24, 27, 28, 33, 34, 37, 39, 44, 49–51, 54, 55, 57–59, 62].

$$\min_x 2x_1 + x_2 + 4x_3 + 3x_4$$

$$\mathcal{X}_1 : x_1 + x_2 + x_3 = 2, \quad \mathcal{X}_2 : x_2 + x_3 - x_4 = 0$$



$$\lambda^1 = (2, 0.5, 2), (x_1, x_2, x_3) \in \mathcal{X}_1$$



$$\lambda^2 = (0.5, 2, 3), (x_2, x_3, x_4) \in \mathcal{X}_2$$

Figure 2. Example decomposition of a binary program into two subproblems, one for each constraint. Each subproblem is represented by a weighted BDD where solid arcs model the cost λ of assigning a 1 to the variable and dashed arcs have 0 cost which model assigning a 0. Optimal assignments w.r.t current (non-optimal) λ are highlighted in green i.e. $x_1 = x_2 = 1, x_3 = 0$ for \mathcal{X}_1 and $x_2 = x_3 = x_4 = 0$ for \mathcal{X}_2 . Our dual update scheme processes multiple variables in parallel which are indicated in same color (e.g. x_1, x_2 in $\mathcal{X}_1, \mathcal{X}_2$ resp.).

Algorithm 1: Parallel Deferred Min-Marginal Averaging

- 1 **input** objective vector $c \in \mathbb{R}^n$, constraint sets $\mathcal{X}_j \subset \{0, 1\}^{\mathcal{I}_j}$ for $j \in [m]$, damping factor $\omega \in (0, 1]$
 - 2 Initialize dual variables $\lambda_i^{j,\beta} = \beta \cdot c_i / |\mathcal{I}_i|$ for all $i \in [n], j \in \mathcal{I}_i$ and $\beta \in \{0, 1\}$.
 - 3 Initialize current and deferred min-marginals $m = \bar{m} = \mathbb{0}$
 - 4 **while** (*stopping criterion not met*) **do**
 - 5 Perform forward pass:
 - 6 **for** $j \in \mathcal{J}$ *in parallel* **do**
 - 7 **for** $i \in \mathcal{I}_j$ *in ascending order* **do**
 - 8 Compute min-marginals for $\beta \in \{0, 1\}$:
 - 9 $m_{ij}^\beta = \min_{x \in \mathcal{X}_j} x^\top \lambda^j \text{ s.t. } x_i = \beta$
 - 10 Update dual variable: $\lambda_i^j \leftarrow \lambda_i^j - \omega \cdot (m_{ij}^1 - m_{ij}^0) + \frac{\omega}{|\mathcal{I}_i|} \sum_{k \in \mathcal{I}_i} (\bar{m}_{kj}^1 - \bar{m}_{kj}^0)$
 - 11 Update deferred min-marginals $\bar{m} \leftarrow m$
 - 12 Perform backward pass analogously:
 - 13 Change ascending variable order into descending
 - 14 **for** $j \in [m], i \in \mathcal{I}_j, \beta \in \{0, 1\}$ **do**
 - 15 Add deferred min-marginals: $\lambda_i^j += \omega(\bar{m}_{ij}^1 - \bar{m}_{ij}^0)$
-

3.3. Parallel Deferred Min-Marginal Averaging

To optimize the dual problem (D), Algorithm 1 iterates in parallel over each subproblem j . For each subproblem, variables are visited in order and min-marginals are computed and stored for updates in the next iteration (lines 8-9). The current min-marginal difference is subtracted and the one from previous iteration is added (line 10) by distributing it equally among subproblems \mathcal{I}_i . Following [59] we use a damping factor $\omega \in (0, 1)$ (0.5 in our experiments) to obtain better final solutions.

Proposition 1. *In each iteration the Lagrange multipliers are feasible and the dual lower bound (D) is non-decreasing.*

The reason for using deferred min-marginals \bar{m} in Algorithm 1 is to make updates separable w.r.t. subproblems and thus enable massive parallelism. Concretely, in the Lagrange variable update (line 10)

$$\lambda_i^j \leftarrow \lambda_i^j - \omega \cdot (m_{ij}^1 - m_{ij}^0) + \underbrace{\frac{\omega}{|\mathcal{I}_i|} \sum_{k \in \mathcal{I}_i} (\bar{m}_{kj}^1 - \bar{m}_{kj}^0)}_{\text{min-marginal averaging}}, \quad (2)$$

the min-marginal averaging step accounts for min-marginals subtracted in previous iteration. If $\bar{m} \leftarrow m$, then (2) matches the update from [37]. Such an update, however, requires coordination among subproblems and thus inefficient for parallel processing. At termination of Alg. 1 we perform a min-marginal averaging step to account for the deferred update from last iteration.

Similar to other dual block coordinate ascent schemes Algorithm 1 can get stuck in suboptimal points, see [58, 59]. As seen in experiments these are usually not far away from the optimum, however.

In Section 5 below we will explain how we can incrementally compute min-marginals reusing previous computations if we represent subproblems as binary decision diagrams. This saves us from computing min-marginals from scratch leading to greater efficiency.

4. Primal Rounding

In order to obtain a primal solution to (BP) from an approximative dual solution to (D) we propose a perturbation method that iteratively changes costs to produce min-marginals across subproblems that are consistent with each other. If all min-marginals agree and favor a single variable, we can reconstruct a primal solution.

Algorithm 2 details our method. If for a variable i all min-marginals indicate that the optimal solution is 0 (resp. 1) Lagrange variables λ are increased (resp. decreased) leaving even more certain min-marginals. In case min-marginals are equal we randomly perturb corresponding λ variables. Lastly, if min-marginals indicate conflicting solutions we compute total min-marginal difference and decide accordingly. In last two cases we add more perturbation to force min-marginals towards non-conflicts. Note that the modified λ variables may not be feasible anymore for (D). For faster convergence we increase the perturbation magnitude after each iteration.

Algorithm 2: Perturbation Primal Rounding

Input: Initial perturbation strength $\delta \in \mathbb{R}_+$,
 perturbation growth rate α , constraint sets
 $\mathcal{X}_j \subset \{0, 1\}^{\mathcal{I}_j}$, Lagrange variables $\lambda \in \mathbb{R}^{\mathcal{I}_j}$

Output: Feasible labeling $x \in \{0, 1\}^n$

- 1 **while** $\exists i \in [n]$ and $j \neq j' \in \mathcal{I}_i$ s.t.
 $\text{sign}(m_{ij}^1 - m_{ij}^0) \neq \text{sign}(m_{ij'}^1 - m_{ij'}^0)$ **do**
- 2 **for** $i = 1, \dots, n$ *in parallel* **do**
- 3 Sample r uniformly from $[-\delta, \delta]$
- 4 **if** $m_{ij}^1 > m_{ij}^0 \forall j \in \mathcal{I}_i$ **then**
- 5 $\lambda_i^j += \delta \forall j \in \mathcal{I}_i$
- 6 **else if** $m_{ij}^1 < m_{ij}^0 \forall j \in \mathcal{I}_i$ **then**
- 7 $\lambda_i^j -= \delta \forall j \in \mathcal{I}_i$
- 8 **else if** $|m_{ij}^1 - m_{ij}^0| = 0 \forall j \in \mathcal{I}_i$ **then**
- 9 $\lambda_i^j += r \cdot \delta \forall j \in \mathcal{I}_i$
- 10 **else**
- 11 Compute total min-marginal difference:
 $d_i = \sum_{j \in \mathcal{I}_i} m_{ij}^1 - m_{ij}^0$
- 12 $\lambda_i^j += \text{sign}(d) \cdot |r| \cdot \delta \forall j \in \mathcal{I}_i$
- 13 Increase perturbation: $\delta \leftarrow \delta \cdot \alpha$
- 14 Reoptimize via Algorithm 1

Remark. The primal rounding scheme in [37] and typical primal ILP heuristics [9] are sequential and build upon sequential operations such as variable propagation. Our primal rounding lends itself to parallelism since we perturb costs on all variables simultaneously and reoptimize via Algorithm 1.

5. Binary Decision Diagrams

As in [37] we use BDDs to represent the feasibility sets $\mathcal{X}_j, j \in [m]$ and compute their min-marginals (MM). BDDs are in essence directed acyclic graphs whose paths between two special nodes (root and terminal) encode all feasible solutions. For a full definition see Appendix.

Definition 4 (BDD). Let an ordered variable set $\mathcal{I} = \{w_1, \dots, w_k\} \subset [n]$ corresponding to a constraint be given. A corresponding BDD is a directed acyclic graph $D = (V, A)$ with

Special nodes: root node r , terminals \perp and \top .

Outgoing Arcs: each node $v \in V \setminus \{\top, \perp\}$ has exactly two successors $s^0(v), s^1(v)$ with outgoing arcs $vs^0(v) \in A$ (the zero arc) and $vs^1(v) \in A$ (the one arc).

Partition: the node set V is partitioned by $\{P_1, \dots, P_k\}, \cup_i P_i = V \setminus \{\top, \perp\}$. Each partition holds all the nodes corresponding to a single variable. It holds that $P_1 = \{r\}$ i.e. it only contains the root node.

Partition Ordering: when $v \in P_i$ then $s^0(v), s^1(v) \in P_{i+1} \cup \{\perp\}$ for $i < k$ and $s^0(v), s^1(v) \in \{\perp, \top\}$ for $v \in P_k$.

Definition 5 (Constraint Set Correspondence). Each BDD defines a constraint set \mathcal{X} via the relation

$$\begin{aligned} \exists (v_1, \dots, v_k, \top) \in \text{Paths}(V, A) \text{ s.t.} \\ x \in \mathcal{X} \Leftrightarrow \begin{aligned} v_1 = r, v_{k+1} = \top, \\ v_{i+1} = s^{x_i}(v_i) \forall i \in [k] \end{aligned} \end{aligned} \quad (3)$$

Thus each path between root r and terminal \top in the BDD corresponds to some feasible variable assignment $x \in \mathcal{X}$.

Figures 2 and 3 illustrate BDD encoding of feasible sets of linear inequalities.

Remark. In the literature [11, 32] BDDs have additional requirements, mainly that there are no isomorphic subgraphs. This allows for some additional canonicity properties like uniqueness and minimality. While all the BDDs in our algorithms satisfy the additional canonicity properties, only what is required in Definition 4 is needed for our purposes, so we keep this simpler setting.

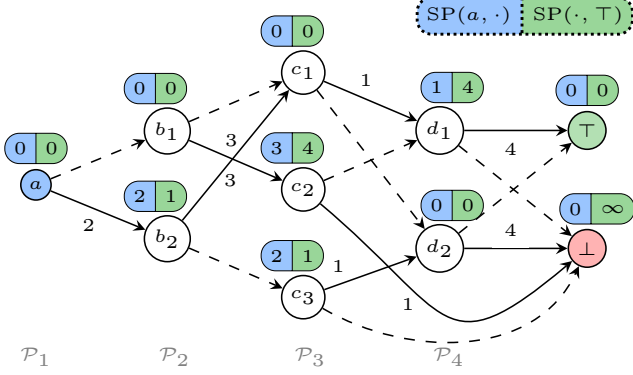


Figure 3. Weighted BDD of a subproblem containing variables: $\mathcal{I} = \{a, b, c, d\}$ with costs (λ): 2, 3, 1, 4 resp. and constraint $a + b - c - d = 0$. Shortest path costs from the root node a and the terminal node \top are shown for each node. Here $\mathcal{P}_1 = \{a\}$, $\mathcal{P}_2 = \{b_1, b_2\}$, $\mathcal{P}_3 = \{c_1, c_2, c_3\}$, $\mathcal{P}_4 = \{d_1, d_2\}$, $s^0(c_2) = d_1$ and $s^1(c_2) = \perp$. Dashed arcs have cost 0 as they model assigning a 0 value to the corresponding variable.

5.1. Efficient Min-Marginal Computation

In order to optimize and compute min-marginals for subproblems we need to consider weighted BDDs.

Definition 6 (Weighted BDD). A weighted BDD is a BDD with arc costs. Let a function $f(x)$ be defined as

$$f(x) = \begin{cases} x^\top \lambda & x \in \mathcal{X} \\ \infty & \text{otherwise} \end{cases} \quad (4)$$

The weighted BDD represents f if it satisfies Def. 5 for the given \mathcal{X} and the arc costs for an $i \in [k]$, $v \in P_i$, $vw \in A$ are set as $\begin{cases} 0 & w \in s^0(v) \\ \lambda_i & w \in s^1(v) \end{cases}$.

Min-marginals for variable $i \in \mathcal{I}$ of a subproblem can be computed by its weighted BDD by calculating shortest path distances from r to all nodes in P_i and shortest path distances from all nodes in P_{i+1} to \top . We use $SP(v, w)$ to denote the shortest path distance between nodes v and w of a weighted BDD. An example shortest path calculation is shown in Figure 3. The min-marginals as defined in (MM) can be computed as

$$m_i^\beta = \min_{\substack{v: s^\beta(v) \in A \\ v \in \mathcal{P}_i}} [SP(r, v) + \beta \cdot \lambda_i + SP(s^\beta(v), \top)] \quad (5)$$

For efficient min-marginal computation in Algorithm 1 we reuse shortest path distances used in (5). Specifically, we replace the lines 8-9 in Alg. 1 by Algs. 3, 4 for the forward and backward pass resp.

Algorithm 3: Forward Pass Min-Marginal Computation

```

1 for  $v \in \mathcal{P}_i$  do
2    $SP(r, v) = \min \left\{ \begin{array}{l} \min_{u: s^0(u)=v} SP(r, u), \\ \min_{u: s^1(u)=v} SP(r, u) + \lambda_i \end{array} \right\}$ 
3 Compute  $m_i^\beta$  via (5)

```

Algorithm 4: Backward Pass Min-Marginal Computation

```

1 for  $v \in \mathcal{P}_{i+1}$  do
2    $SP(v, \top) = \min \left\{ \begin{array}{l} SP(s^0(v), \top), \\ SP(s^1(v), \top) + \lambda_{i+1} \end{array} \right\}$ 
3 Compute  $m_i^\beta$  via (5)

```

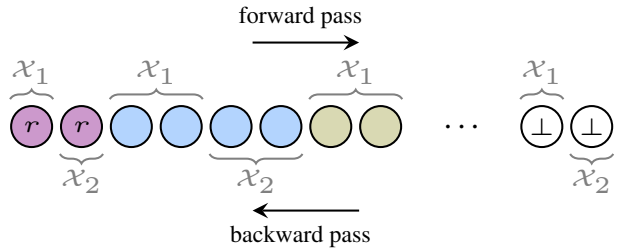


Figure 4. Arrangement of BDD nodes in GPU memory for the ILP in Figure 2. For the forward pass in Alg. 1 we proceed from root to terminal nodes and vice versa for the backward pass.

Efficient GPU implementation In addition to solving all subproblems in parallel, we also exploit parallelism within each subproblem during shortest path updates. Specifically in Alg. 3, we parallelize over all $v \in \mathcal{P}_i$ and perform the min operation atomically. Similarly in Alg. 4 we parallelize over all $v \in \mathcal{P}_{i+1}$ but without requiring atomic update.

To enable fast GPU memory access via memory coalescing we arrange BDD nodes in the following fashion. First, all nodes within a BDD which belong to the same partition \mathcal{P} are laid out consecutively. Secondly, across different BDDs, nodes are ordered w.r.t increasing hop distance from their corresponding root nodes. Such arrangement for the ILP in Figure 2 is shown in Figure 4.

6. Experiments

We show effectiveness of our solver against a state-of-the-art ILP solver, the general purpose BDD-based solver [37] and specialized CPU solvers for specific problem classes. We have chosen the largest structured prediction ILPs we are aware of in the literature that are publicly available. Our results are computed on a single NVIDIA Volta V100 (16GB) GPU unless stated otherwise. For CPU solvers we use AMD

| | Cell tracking | | Graph matching | | | MRF | | | | QAPLib | |
|---|-----------------|-----------------|-----------------|-----------------|-----------------|----------------|-----------------|-----------------|-----------------|----------------|----------------|
| | Small | Large | Hotel | House | Worms | C-seg | C-seg-n4 | C-seg-n8 | Obj-seg | Small | Large |
| # instances | 10 | 5 | 105 | 105 | 30 | 3 | 9 | 9 | 5 | 105 | 29 |
| n_{max} | 1.2M | 10M | 0.3M | 0.3M | 1.5M | 3.3M | 1.2M | 1.4M | 681k | 3M | 49M |
| m_{max} | 0.2M | 2.3M | 52k | 52k | 0.2M | 13.6M | 4.2M | 8.3M | 2.2M | 245k | 2M |
| Dual objective (lower bound) \uparrow | | | | | | | | | | | |
| Gurobi [20] | -4.382e6 | -1.545e8 | -4.293e3 | -3.778e3 | -4.849e4 | 3.085e8 | 1.9757e4 | 1.9729e4 | 3.1311e4 | 2.913e6 | 4.512e4 |
| BDD-CPU [37] | -4.387e6 | -1.549e8 | -4.293e3 | -3.778e3 | -4.878e4 | 3.085e8 | 1.9643e4 | 1.9631e4 | 3.1248e4 | 3.675e6 | 8.172e6 |
| Specialized | -4.385e6 | -1.551e8 | -4.293e3 | -3.778e3 | -4.847e4 | 3.085e8 | 2.0012e4 | 1.9991e4 | 3.1317e4 | - | - |
| FastDOG | -4.387e6 | -1.549e8 | -4.293e3 | -3.778e3 | -4.893e4 | 3.085e8 | 2.0011e4 | 1.9990e4 | 3.1317e4 | 3.747e6 | 8.924e6 |
| Primal objective (upper bound) \downarrow | | | | | | | | | | | |
| Gurobi [20] | -4.382e6 | -1.524e8 | -4.293e3 | -3.778e3 | -4.842e4 | 3.085e8 | 2.8464e4 | 2.7829e4 | 1.4981e5 | 5.186e7 | 1.431e8 |
| BDD-CPU [37] | -4.337e6 | -1.515e8 | -4.293e3 | -3.778e3 | -4.783e4 | 3.086e8 | 2.1781e4 | 2.2338e4 | 3.1525e4 | 5.239e7 | 1.452e8 |
| Specialized | -4.361e6 | -1.531e8 | -4.293e3 | -3.778e3 | -4.845e4 | 3.085e8 | 2.0012e4 | 1.9991e4 | 3.1317e4 | - | - |
| FastDOG | -4.376e6 | -1.541e8 | -4.293e3 | -3.778e3 | -4.831e4 | 3.085e8 | 2.0016e4 | 1.9995e4 | 3.1322e4 | 4.330e7 | 1.376e8 |
| Runtimes [s] \downarrow | | | | | | | | | | | |
| Gurobi [20] | 1 | 1584 | 4 | 7 | 1048 | 132 | 980 | 1337 | 1506 | 3948 | 6742 |
| BDD-CPU [37] | 14 | 216 | 6 | 12 | 528 | 70 | 107 | 218 | 232 | 357 | 5952 |
| Specialized | 1.5 | 90 | 3 | 3 | 214 | 155 | 9 | 30 | 3 | - | - |
| FastDOG | 13 | 110 | 0.2 | 0.4 | 54 | 14 | 9 | 13 | 39 | 137 | 6928 |

Table 2. Results comparison on all datasets. For each dataset, the results on corresponding specialized solvers are computed using [21,31,51]. Numbers in bold highlight the best performance. n_{max}, m_{max} : Maximum number of variables, constraints in the category.

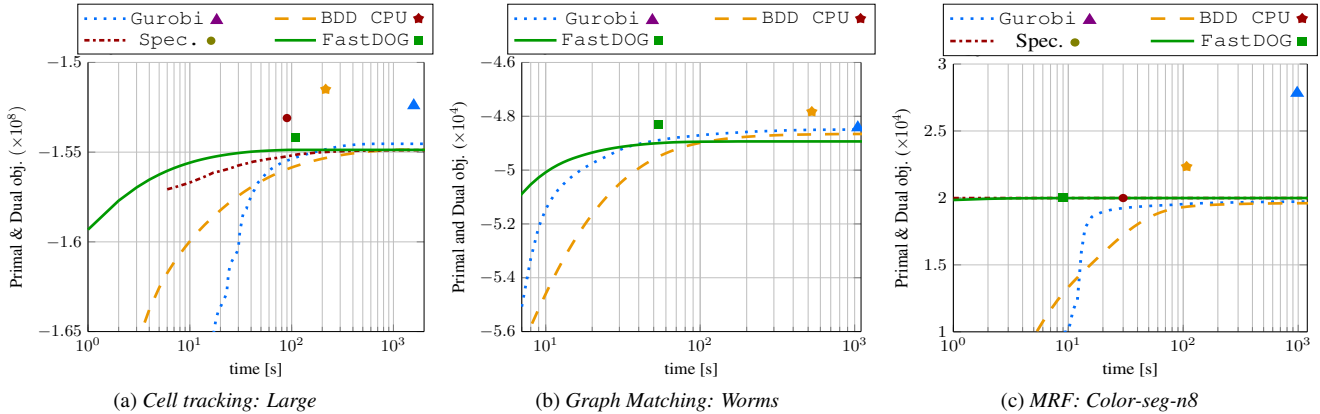


Figure 5. Convergence plots averaged over all instances of a dataset. Lower curves depict increasing lower bounds while markers denote objectives of rounded primal solutions. The x-axis is plotted logarithmically.

EPYC 7702 CPU.

Datasets Our benchmark problems can be categorized as follows.

Cell tracking: Instances from [21] which we partition into small and large instances as also done in [37].

Graph matching (GM): Quadratic assignment problems (often called graph matching in the literature) for correspondence in computer vision [53] (hotel, house) and developmental biology [29] (worms).

Markov Random Field (MRF): Several datasets from the OpenGM [30] benchmark, containing both small and

large instances with varying topologies and number of labels. We have chosen the datasets *color-seg*, *color-seg-n4*, *color-seg-n8* and *object-seg*.

QAPLib: The widely used benchmark dataset for quadratic assignment problems used in the combinatorial optimization community [12]. We partition QAPLib instances into small (up to 50 vertices) and large (up to 128 vertices) instances. For large instances we use NVIDIA RTX 8000 (48GB) GPU.

Algorithms We compare results on the following algorithms.

Gurobi: The commercial ILP solver [20] as reported in [37]. The barrier method is used for QAPLib and dual simplex for all other datasets.

BDD-CPU: BDD-based min-marginal averaging approach of [37]. The algorithm runs on CPU with 16 threads for parallelization. Primal solutions are rounded using their BDD-based depth-first search scheme.

Specialized solvers: State-of-the-art problem specific solver for each dataset. For cell-tracking we use the solver from [21], the AMP solver for graph matching proposed in [51] and TRWS for MRF [33].

FastDOG: Our approach where for the GPU implementation we use the CUDA [41] and Thrust [22] programming frameworks. For rounding primal solutions with Algorithm 2 we set $\delta = 1.0$ for the initial perturbation and $\alpha = 1.2$ for the perturbation growth rate. For constructing BDDs out of linear (in)equalities we use the same approach as for BDD-CPU.

For *MRF*, parallel algorithms such as [54] exist however TRWS is faster on the sparse problems we consider. While we are aware of even faster purely primal heuristics [10,35] for *MRF* and e.g. [26] for *graph matching* they do not optimize a convex relaxation and hence do not provide lower bounds. Hence, we have chosen TRWS [33] for *MRF* and AMP [51] for *graph matching* which, similar to FastDOG, optimize an equivalent resp. similar Lagrange decomposition and hence can be directly compared.

Results In Table 2 we show aggregated results over all instances of each specific benchmark dataset. Runtimes are taken w.r.t. computation of both primal and dual bounds. A more detailed table with results for each instance is given in the Appendix.

In Figure 5 we show averaged convergence plots for various solvers. In general we offer a very good anytime performance producing at most times and in general during the beginning better lower bounds than our baselines.

Discussion In general, we are always faster (up to a factor of 10) than BDD-CPU [37] and except on *worms* we achieve similar or better lower bounds. In comparison to the respective hand-crafted Specialized CPU solvers we also achieve comparable runtimes with comparable lower and upper bounds. While Gurobi achieves, if given unlimited time, better lower bounds and primal solutions, our FastDOG solver outperforms it on the larger instances when we abort Gurobi early after hitting a time limit. We argue that we outperform Gurobi on larger instances due to its superlinear iteration complexity.

When comparing the number of dual iterations to BDD-CPU we need roughly 3-times as many to reach the

same lower bound. Hence, when counting the number of arithmetic operations FastDOG is less efficient in terms of dual improvement per iteration than BDD-CPU which performs sequential updates. Nonetheless, as we can perform more iterations per second this still leads to an overall faster algorithm.

Since we are solving a relaxation thus the lower bounds and quality of primal solutions are dependent on the tightness of this relaxation. For all datasets except QAPLib our (and also baselines’) lower and upper bounds are fairly close, reflecting the nature of commonly occurring structured prediction problems.

7. Conclusion

We have proposed a massively parallelizable generic algorithm that can solve a wide variety of ILPs on GPU. Our results indicate that the performance of specialized efficient CPU solvers can be matched or even surpassed by a completely generic GPU solver. Our implementation is a first prototype and we conjecture that more speedups can be gained by elaborate implementation techniques, e.g. compression of the BDD representation, better memory layout for better memory coalescing, multi-GPU support etc. We argue that future improvements in optimization algorithms for structured prediction can be made by developing GPU friendly problem specific solvers and with improvements in our or other generic GPU solvers that can benefit many problem classes simultaneously.

References

- [1] Ahmed Abbas and Paul Swoboda. RAMA: A Rapid Multicut Algorithm on GPU. *arXiv preprint arXiv:2109.01838*, 2021. 1, 2, 3
- [2] Henrik Reif Andersen, Tarik Hadzic, John N Hooker, and Peter Tiedemann. A constraint store based on multivalued decision diagrams. In *International Conference on Principles and Practice of Constraint Programming*, pages 118–132. Springer, 2007. 3
- [3] Chetan Arora and Amir Globerson. Higher order matching for consistent multiple target tracking. In *Proceedings of the IEEE International Conference on Computer Vision*, pages 177–184, 2013. 3
- [4] David Bergman and Andre A. Cire. Decomposition based on decision diagrams. In Claude-Guy Quimper, editor, *Integration of AI and OR Techniques in Constraint Programming*, pages 45–54, Cham, 2016. Springer International Publishing. 3
- [5] David Bergman and Andre A Cire. Discrete nonlinear optimization by state-space decompositions. *Management Science*, 64(10):4700–4720, 2018. 3
- [6] David Bergman, Andre A Cire, and Willem-Jan van Hoeve. Lagrangian bounds from decision diagrams. *Constraints*, 20(3):346–361, 2015. 3

- [7] David Bergman, Andre A Cire, Willem-Jan Van Hoeve, and John Hooker. *Decision diagrams for optimization*, volume 1. Springer, 2016. 3
- [8] David Bergman, Andre A Cire, Willem-Jan van Hoeve, and John N Hooker. Discrete optimization with decision diagrams. *INFORMS Journal on Computing*, 28(1):47–66, 2016. 3
- [9] Timo Berthold. Primal heuristics for mixed integer programs. 2006. 5
- [10] Yuri Boykov, Olga Veksler, and Ramin Zabih. Fast approximate energy minimization via graph cuts. *IEEE Transactions on pattern analysis and machine intelligence*, 23(11):1222–1239, 2001. 8
- [11] Randal E Bryant. Graph-based algorithms for boolean function manipulation. *Computers, IEEE Transactions on*, 100(8):677–691, 1986. 5, 12
- [12] Rainer E Burkard, Stefan E Karisch, and Franz Rendl. QAPLIB—a quadratic assignment problem library. *Journal of Global optimization*, 10(4):391–403, 1997. 7
- [13] Margarita P Castro, Andre A Cire, and J Christopher Beck. An mdd-based lagrangian approach to the multicommodity pickup-and-delivery tsp. *INFORMS Journal on Computing*, 32(2):263–278, 2020. 3
- [14] Cplex, IBM ILOG. CPLEX optimization studio 12.10, 2019. 1, 2
- [15] Maxime Gasse, Didier Chételat, Nicola Ferroni, Laurent Charlin, and Andrea Lodi. Exact combinatorial optimization with graph convolutional neural networks. *arXiv preprint arXiv:1906.01629*, 2019. 2
- [16] Amir Globerson and Tommi S Jaakkola. Fixing max-product: Convergent message passing algorithms for MAP LP-relaxations. In *Advances in neural information processing systems*, pages 553–560, 2008. 2, 3
- [17] Jacek Gondzio and Robert Sarkissian. Parallel interior-point solver for structured linear programs. *Mathematical Programming*, 96(3):561–584, 2003. 2
- [18] Jaime E González, Andre A Cire, Andrea Lodi, and Louis-Martin Rousseau. BDD-based optimization for the quadratic stable set problem. *Discrete Optimization*, page 100610, 2020. 3
- [19] Jaime E González, Andre A Cire, Andrea Lodi, and Louis-Martin Rousseau. Integrated integer programming and decision diagram search tree with an application to the maximum independent set problem. *Constraints*, pages 1–24, 2020. 3
- [20] Gurobi Optimization, LLC. Gurobi Optimizer Reference Manual, 2021. 1, 2, 7, 8
- [21] Stefan Haller, Mangal Prakash, Lisa Hutschenreiter, Tobias Pietzsch, Carsten Rother, Florian Jug, Paul Swoboda, and Bogdan Savchynskyy. A primal-dual solver for large-scale tracking-by-assignment. In *AISTATS*, 2020. 2, 3, 7, 8
- [22] Jared Hoberock and Nathan Bell. Thrust: A parallel template library, 2010. Version 1.7.0. 8
- [23] John N. Hooker. Improved job sequencing bounds from decision diagrams. In Thomas Schiex and Simon de Givry, editors, *Principles and Practice of Constraint Programming*, pages 268–283, Cham, 2019. Springer International Publishing. 3
- [24] Andrea Hornakova, Timo Kaiser, Paul Swoboda, Michal Rolinek, Bodo Rosenhahn, and Roberto Henschel. Making higher order MOT scalable: An efficient approximate solver for lifted disjoint paths. In *Proceedings of the IEEE/CVF International Conference on Computer Vision*, pages 6330–6340, 2021. 2, 3
- [25] Qi Huangfu and J. A. J. Hall. Parallelizing the dual revised simplex method. *Math. Program. Comput.*, 10(1):119–142, 2018. 2
- [26] Lisa Hutschenreiter, Stefan Haller, Lorenz Feineis, Carsten Rother, Dagmar Kainmüller, and Bogdan Savchynskyy. Fusion moves for graph matching. 2021. 8
- [27] Jeremy Jancsary and Gerald Matz. Convergent decomposition solvers for tree-reweighted free energies. In *Proceedings of the Fourteenth International Conference on Artificial Intelligence and Statistics*, pages 388–398, 2011. 2, 3
- [28] Jason K Johnson, Dmitry M Malioutov, and Alan S Willsky. Lagrangian relaxation for MAP estimation in graphical models. *arXiv preprint arXiv:0710.0013*, 2007. 2, 3
- [29] Dagmar Kainmueller, Florian Jug, Carsten Rother, and Gene Myers. Active graph matching for automatic joint segmentation and annotation of *C. elegans*. In *International Conference on Medical Image Computing and Computer-Assisted Intervention*, pages 81–88. Springer, 2014. 7
- [30] Jörg H. Kappes, Björn Andres, Fred A. Hamprecht, Christoph Schnörr, Sebastian Nowozin, Dhruv Batra, Sungwoong Kim, Bernhard X. Kausler, Thorben Kröger, Jan Lellmann, Nikos Komodakis, Bogdan Savchynskyy, and Carsten Rother. A comparative study of modern inference techniques for structured discrete energy minimization problems. *International Journal of Computer Vision*, 115(2):155–184, 2015. 1, 2, 7
- [31] Jörg Hendrik Kappes, Markus Speth, Gerhard Reinelt, and Christoph Schnörr. Towards efficient and exact MAP-inference for large scale discrete computer vision problems via combinatorial optimization. In *2013 IEEE Conference on Computer Vision and Pattern Recognition*, pages 1752–1758, 2013. 7
- [32] Donald E Knuth. *The art of computer programming, volume 4A: combinatorial algorithms, part 1*. Pearson Education India, 2011. 5
- [33] Vladimir Kolmogorov. Convergent tree-reweighted message passing for energy minimization. *IEEE transactions on pattern analysis and machine intelligence*, 28(10):1568–1583, 2006. 2, 3, 8
- [34] Vladimir Kolmogorov. A new look at reweighted message passing. *IEEE transactions on pattern analysis and machine intelligence*, 37(5):919–930, 2014. 2, 3
- [35] Nikos Komodakis and Georgios Tziritas. Approximate labeling via graph cuts based on linear programming. *IEEE transactions on pattern analysis and machine intelligence*, 29(8):1436–1453, 2007. 8
- [36] Jan-Hendrik Lange, Andreas Karrenbauer, and Bjoern Andres. Partial optimality and fast lower bounds for weighted correlation clustering. In *International Conference on Machine Learning*, pages 2892–2901. PMLR, 2018. 2
- [37] Jan-Hendrik Lange and Paul Swoboda. Efficient message passing for 0–1 ILPs with binary decision diagrams. In *International Conference on Machine Learning*, pages 6000–6010. PMLR, 2021. 1, 2, 3, 4, 5, 6, 7, 8, 12

- [38] Leonardo Lozano, David Bergman, and J Cole Smith. On the consistent path problem. *Optimization Online e-prints*, 2018. [3](#)
- [39] Talya Meltzer, Amir Globerson, and Yair Weiss. Convergent message passing algorithms—a unifying view. *arXiv preprint arXiv:1205.2625*, 2012. [2](#), [3](#)
- [40] Vinod Nair, Sergey Bartunov, Felix Gimeno, Ingrid von Glehn, Pawel Lichocki, Ivan Lobov, Brendan O’Donoghue, Nicolas Sonnerat, Christian Tjandraatmadja, Pengming Wang, et al. Solving mixed integer programs using neural networks. *arXiv preprint arXiv:2012.13349*, 2020. [2](#)
- [41] NVIDIA, Péter Vingelmann, and Frank H.P. Fitzek. CUDA, release: 11.2, 2021. [8](#)
- [42] Kalyan Perumalla and Maksudul Alam. Design Considerations for GPU-Based Mixed Integer Programming on Parallel Computing Platforms. Association for Computing Machinery, New York, NY, USA, 2021. [1](#), [2](#)
- [43] Ted Ralphs, Yuji Shinano, Timo Berthold, and Thorsten Koch. Parallel solvers for mixed integer linear optimization. In *Handbook of parallel constraint reasoning*, pages 283–336. Springer, 2018. [2](#)
- [44] B. Savchynskyy, S. Schmidt, Jörg H. Kappes, and Christoph Schnörr. Efficient MRF energy minimization via adaptive diminishing smoothing. *UAI. Proceedings*, pages 746–755, 2012. [1](#), [2](#), [3](#)
- [45] Alexander Shekhovtsov, Christian Reinbacher, Gottfried Graber, and Thomas Pock. Solving dense image matching in real-time using discrete-continuous optimization. In *Proceedings of the 21st Computer Vision Winter Workshop (CVWW)*, page 13, 2016. [1](#), [2](#)
- [46] Edmund Smith, Jacek Gondzio, and Julian Hall. GPU acceleration of the matrix-free interior point method. In Roman Wyrzykowski, Jack Dongarra, Konrad Karczewski, and Jerzy Waśniewski, editors, *Parallel Processing and Applied Mathematics*, pages 681–689, Berlin, Heidelberg, 2012. Springer Berlin Heidelberg. [2](#)
- [47] Boro Sofranac, Ambros Gleixner, and Sebastian Pokutta. Accelerating domain propagation: an efficient GPU-parallel algorithm over sparse matrices. In *2020 IEEE/ACM 10th Workshop on Irregular Applications: Architectures and Algorithms (IA3)*, pages 1–11. IEEE, 2020. [2](#)
- [48] Nicolas Sonnerat, Pengming Wang, Ira Ktena, Sergey Bartunov, and Vinod Nair. Learning a large neighborhood search algorithm for mixed integer programs. *arXiv preprint arXiv:2107.10201*, 2021. [2](#)
- [49] Paul Swoboda and Bjoern Andres. A message passing algorithm for the minimum cost multicut problem. In *Proceedings of the IEEE Conference on Computer Vision and Pattern Recognition*, pages 1617–1626, 2017. [2](#), [3](#)
- [50] Paul Swoboda, Ashkan Mokarian, Christian Theobalt, Florian Bernard, et al. A convex relaxation for multi-graph matching. In *Proceedings of the IEEE Conference on Computer Vision and Pattern Recognition*, pages 11156–11165, 2019. [2](#), [3](#)
- [51] Paul Swoboda, Carsten Rother, Hassan Abu Alhaja, Dagmar Kainmuller, and Bogdan Savchynskyy. A study of lagrangean decompositions and dual ascent solvers for graph matching. In *Proceedings of the IEEE Conference on Computer Vision and Pattern Recognition*, pages 1607–1616, 2017. [2](#), [3](#), [7](#), [8](#)
- [52] Christian Tjandraatmadja and Willem-Jan van Hoeve. Incorporating bounds from decision diagrams into integer programming. *Mathematical Programming Computation*, pages 1–32, 2020. [3](#)
- [53] Lorenzo Torresani, Vladimir Kolmogorov, and Carsten Rother. Feature correspondence via graph matching: Models and global optimization. In *European conference on computer vision*, pages 596–609. Springer, 2008. [7](#)
- [54] Siddharth Tourani, Alexander Shekhovtsov, Carsten Rother, and Bogdan Savchynskyy. MPLP++: Fast, parallel dual block-coordinate ascent for dense graphical models. In *Proceedings of the European Conference on Computer Vision (ECCV)*, pages 251–267, 2018. [1](#), [2](#), [3](#), [8](#)
- [55] Siddharth Tourani, Alexander Shekhovtsov, Carsten Rother, and Bogdan Savchynskyy. Taxonomy of dual block-coordinate ascent methods for discrete energy minimization. In *AISTATS*, 2020. [2](#), [3](#)
- [56] Vibhav Vineet and PJ Narayanan. CUDA cuts: Fast graph cuts on the GPU. In *2008 IEEE Computer Society Conference on Computer Vision and Pattern Recognition Workshops*, pages 1–8. IEEE, 2008. [2](#)
- [57] Huayan Wang and Daphne Koller. Subproblem-tree calibration: A unified approach to max-product message passing. In *ICML (2)*, pages 190–198, 2013. [2](#), [3](#)
- [58] Tomas Werner. A linear programming approach to max-sum problem: A review. *IEEE transactions on pattern analysis and machine intelligence*, 29(7):1165–1179, 2007. [2](#), [3](#), [5](#)
- [59] Tomáš Werner, Daniel Průša, and Tomáš Dlask. Relative interior rule in block-coordinate descent. In *Proceedings of the IEEE International Conference on Computer Vision*, 2020. To appear. [3](#), [4](#), [5](#)
- [60] Jiadong Wu, Zhengyu He, and Bo Hong. Chapter 5 - efficient CUDA algorithms for the maximum network flow problem. In Wen mei W. Hwu, editor, *GPU Computing Gems Jade Edition*, Applications of GPU Computing Series, pages 55–66. Morgan Kaufmann, Boston, 2012. [2](#)
- [61] Zhiwei Xu, Thalaiyasingam Ajanthan, and Richard Hartley. Fast and differentiable message passing on pairwise markov random fields. In *Proceedings of the Asian Conference on Computer Vision*, 2020. [1](#), [2](#)
- [62] Zhen Zhang, Qinfeng Shi, Julian McAuley, Wei Wei, Yanming Zhang, and Anton Van Den Hengel. Pairwise matching through max-weight bipartite belief propagation. In *Proceedings of the IEEE Conference on Computer Vision and Pattern Recognition*, pages 1202–1210, 2016. [2](#), [3](#)

Appendix

8. Proof of Proposition 1

Proof.

Feasibility of iterates We prove

$$\sum_{j \in \mathcal{J}} \lambda_i^j + \omega \cdot (m_{ji}^1 - m_{ji}^0) = c_i \quad (6)$$

just before line 11 in Algorithm 1. We do an inductive proof over the number of iterates.

iter = 0: Follows from $\bar{m} = 0$ and the uniform distribution of costs in line 3 of Algorithm 1.

iter > 0: Let λ, m, \bar{m} be last iterations' Lagrange multipliers, min-marginals and (deferred) min-marginals. Also let λ', m' and \bar{m}' be the same from current iteration just before line 11. Note that $\bar{m}' = m$. It holds that

$$\sum_{j \in \mathcal{J}_i} \left[\lambda_i'^j + \omega \cdot (m_{ji}^1 - m_{ji}^0) \right] = \sum_{j \in \mathcal{J}_i} \left[\lambda_i^j - \omega(m_{ij}^1 - m_{ij}^0) + \sum_{k \in \mathcal{J}_i} \left(\frac{\omega}{|\mathcal{J}_i|} (m_{ik}^1 - m_{ik}^0) \right) + \omega \cdot (m_{ji}^1 - m_{ji}^0) \right] \quad (7a)$$

$$= \sum_{j \in \mathcal{J}_i} \left[\lambda_i^j + \omega \cdot (m_{ij}^1 - m_{ij}^0) \right] \quad (7b)$$

$$= c_i. \quad (7c)$$

Non-decreasing Lower Bound In order to prove that iterates have non-decreasing lower bound we will consider an equivalent lifted representation in which proving the non-decreasing lower bound will be easier.

Lifted Representation Introduce $\lambda_i^{j,\beta}$ for $\beta \in \{0, 1\}$ and the subproblems

$$E(\lambda^{j,1}, \lambda^{j,0}) = \min_{x \in \mathcal{X}_j} \langle x, \lambda^{j,1} \rangle + \langle 1 - x, \lambda^{j,0} \rangle \quad (8)$$

Then (D) is equivalent to

$$\max_{\lambda^1, \lambda^0} \sum_{j \in \mathcal{J}} E(\lambda^{j,1}, \lambda^{j,0}) \text{ s.t. } \sum_{j \in \mathcal{J}_i} \lambda_i^{j,\beta} = \beta \cdot c_i \quad (9)$$

We have the transformation from original to lifted λ

$$\lambda \mapsto (\lambda^1 \leftarrow \lambda, \lambda^0 \leftarrow 0) \quad (10)$$

and from lifted to original λ

$$(\lambda^1, \lambda^0) \mapsto \lambda^1 - \lambda^0. \quad (11)$$

It can be easily shown that the lower bounds are invariant under the above mappings and feasible λ for (D) are mapped to feasible ones for (9) and vice versa.

The update rule line 10 in Algorithm 1 for the lifted representation can be written as

$$\lambda_i^{j,\beta} \leftarrow \lambda_i^{j,\beta} - \omega \cdot \min(m_{ij}^\beta - m_{ij}^{1-\beta}, 0) + \omega \cdot \min(\bar{m}_{ij}^\beta - \bar{m}_{ij}^{1-\beta}, 0) \quad (12)$$

It can be easily shown that (12) and line 10 in Algorithm 1 are corresponding to each other under the transformation from lifted to original λ .

Continuation of Non-decreasing Lower Bound Define

$$\lambda_i'^{j,\beta} = \lambda_i^j - \omega \cdot \min(m_{ij}^\beta - m_{ij}^{1-\beta}, 0). \quad (13)$$

Then $E(\lambda'^{j,1}, \lambda'^{j,0}) = E(\lambda^{j,1}, \lambda^{j,0})$ are equal due to the definition of min-marginals. Define next

$$\lambda_i''^{j,\beta} = \lambda_i'^{j,\beta} + \omega \cdot \min(\bar{m}_{ij}^\beta - \bar{m}_{ij}^{1-\beta}, 0). \quad (14)$$

Then $E(\lambda''^{j,1}, \lambda''^{j,0}) \geq E(\lambda'^{j,1}, \lambda'^{j,0})$ since $\lambda'' \geq \lambda'$. This proves the claim. \square

9. BDDs

We use reduced ordered binary decision diagrams [11] as also done in [37]. For more details see [37].

10. Detailed results

10.1. Cell tracking

Table 3. Detailed results of FastDOG on *Cell tracking - small dataset*

| | LB \uparrow | LB time [s] | UB \downarrow | UB time [s] |
|--------------------|---------------|-------------|-----------------|-------------|
| MEAN | -4387353 | 3 | -4376244 | 10.34 |
| DIC-C2DH-HeLA | -3435189 | 3.5 | -3404116 | 9.43 |
| drosophila | -12972321 | 1.7 | -12971663 | 2.54 |
| Fluo-C2DL-MS-01 | -2702746 | 7 | -2680328 | 26.49 |
| Fluo-C2DL-MS-02 | -2902893 | 1 | -2899711 | 5.93 |
| Fluo-N2DH-GOWT1-01 | -6722103 | 0.3 | -6719992 | 3.11 |
| Fluo-N2DH-GOWT1-02 | -8480162 | 0.8 | -8477563 | 6.18 |
| Fluo-N2DL-HELA | -4045972 | 6.5 | -4034819 | 30.97 |
| flywing-11 | -98500 | 3.3 | -98280 | 3.03 |
| PhC-C2DH-U373-01 | -1529164 | 3.7 | -1519372 | 7.12 |
| PhC-C2DH-U373-02 | -984484 | 2.1 | -956599 | 8.58 |

Table 4. Detailed results of FastDOG on *Cell tracking - large dataset*

| | LB \uparrow | LB time [s] | UB \downarrow | UB time [s] |
|-----------------|---------------|-------------|-----------------|-------------|
| MEAN | -154874000 | 39 | -154171050 | 71.49 |
| flywing-100-1 | -101971727 | 38.9 | -101644067 | 57.78 |
| flywing-100-2 | -102464774 | 41 | -102144340 | 52.43 |
| flywing-245 | -386543634 | 93.5 | -383920619 | 160.53 |
| PhC-C2DL-PSC-01 | -96025589 | 13.1 | -95881123 | 52.82 |
| PhC-C2DL-PSC-02 | -87364274 | 8.7 | -87265102 | 33.89 |

10.2. Graph matching

Table 5. Detailed results of FastDOG on *Graph matching - hotel dataset*

| | LB \uparrow | LB time [s] | UB \downarrow | UB time [s] |
|-----------------------------|---------------|-------------|-----------------|-------------|
| MEAN | -4293 | 0.2 | -4293 | 0.01 |
| energy-hotel-frame15frame22 | -4598 | 0.2 | -4598 | 0.01 |
| energy-hotel-frame15frame29 | -4540 | 0.1 | -4540 | 0.01 |
| energy-hotel-frame15frame36 | -4481 | 0.2 | -4481 | 0.01 |
| energy-hotel-frame15frame43 | -4377 | 0.2 | -4377 | 0.01 |
| energy-hotel-frame15frame50 | -4294 | 0.2 | -4294 | 0.01 |
| energy-hotel-frame15frame57 | -4244 | 0.2 | -4244 | 0.01 |
| energy-hotel-frame15frame64 | -4172 | 0.2 | -4172 | 0.01 |
| energy-hotel-frame15frame71 | -4135 | 0.2 | -4135 | 0.01 |
| energy-hotel-frame15frame78 | -4036 | 0.2 | -4036 | 0.01 |

Continued on next page

Table 5 Continued from previous page

| | LB \uparrow | LB time [s] | UB \downarrow | UB time [s] |
|-----------------------------|---------------|-------------|-----------------|-------------|
| energy-hotel-frame15frame85 | -3985 | 0.2 | -3985 | 0.01 |
| energy-hotel-frame15frame92 | -3898 | 0.2 | -3898 | 0.01 |
| energy-hotel-frame15frame99 | -3860 | 0.2 | -3860 | 0.01 |
| energy-hotel-frame1frame15 | -4498 | 0.2 | -4498 | 0.01 |
| energy-hotel-frame1frame22 | -4438 | 0.1 | -4438 | 0.01 |
| energy-hotel-frame1frame29 | -4368 | 0.2 | -4368 | 0.01 |
| energy-hotel-frame1frame36 | -4306 | 0.2 | -4306 | 0.01 |
| energy-hotel-frame1frame43 | -4194 | 0.2 | -4194 | 0.01 |
| energy-hotel-frame1frame50 | -4125 | 0.2 | -4125 | 0.01 |
| energy-hotel-frame1frame57 | -4064 | 0.2 | -4064 | 0.01 |
| energy-hotel-frame1frame64 | -4021 | 0.2 | -4021 | 0.01 |
| energy-hotel-frame1frame71 | -3969 | 0.2 | -3969 | 0.01 |
| energy-hotel-frame1frame78 | -3874 | 0.2 | -3874 | 0.01 |
| energy-hotel-frame1frame85 | -3817 | 0.2 | -3817 | 0.01 |
| energy-hotel-frame1frame8 | -4570 | 0.1 | -4570 | 0.01 |
| energy-hotel-frame1frame92 | -3728 | 0.3 | -3728 | 0.01 |
| energy-hotel-frame1frame99 | -3691 | 0.4 | -3691 | 0.01 |
| energy-hotel-frame22frame29 | -4615 | 0.1 | -4615 | 0.01 |
| energy-hotel-frame22frame36 | -4527 | 0.2 | -4527 | 0.01 |
| energy-hotel-frame22frame43 | -4428 | 0.2 | -4428 | 0.01 |
| energy-hotel-frame22frame50 | -4343 | 0.2 | -4343 | 0.01 |
| energy-hotel-frame22frame57 | -4302 | 0.2 | -4302 | 0.01 |
| energy-hotel-frame22frame64 | -4219 | 0.2 | -4219 | 0.01 |
| energy-hotel-frame22frame71 | -4188 | 0.2 | -4188 | 0.01 |
| energy-hotel-frame22frame78 | -4109 | 0.2 | -4109 | 0.01 |
| energy-hotel-frame22frame85 | -4063 | 0.2 | -4063 | 0.01 |
| energy-hotel-frame22frame92 | -3979 | 0.2 | -3979 | 0.01 |
| energy-hotel-frame22frame99 | -3956 | 0.2 | -3956 | 0.01 |
| energy-hotel-frame29frame36 | -4605 | 0.1 | -4605 | 0.01 |
| energy-hotel-frame29frame43 | -4493 | 0.1 | -4493 | 0.01 |
| energy-hotel-frame29frame50 | -4408 | 0.2 | -4408 | 0.01 |
| energy-hotel-frame29frame57 | -4373 | 0.2 | -4373 | 0.01 |
| energy-hotel-frame29frame64 | -4295 | 0.2 | -4295 | 0.01 |
| energy-hotel-frame29frame71 | -4253 | 0.2 | -4253 | 0.01 |
| energy-hotel-frame29frame78 | -4167 | 0.2 | -4167 | 0.01 |
| energy-hotel-frame29frame85 | -4118 | 0.2 | -4118 | 0.01 |
| energy-hotel-frame29frame92 | -4037 | 0.2 | -4037 | 0.01 |
| energy-hotel-frame29frame99 | -4007 | 0.2 | -4007 | 0.01 |
| energy-hotel-frame36frame43 | -4571 | 0.1 | -4571 | 0.01 |
| energy-hotel-frame36frame50 | -4489 | 0.2 | -4489 | 0.01 |
| energy-hotel-frame36frame57 | -4451 | 0.2 | -4451 | 0.01 |
| energy-hotel-frame36frame64 | -4373 | 0.2 | -4373 | 0.01 |
| energy-hotel-frame36frame71 | -4326 | 0.2 | -4326 | 0.01 |
| energy-hotel-frame36frame78 | -4249 | 0.2 | -4249 | 0.01 |
| energy-hotel-frame36frame85 | -4192 | 0.2 | -4192 | 0.01 |
| energy-hotel-frame36frame92 | -4124 | 0.2 | -4124 | 0.01 |
| energy-hotel-frame36frame99 | -4094 | 0.2 | -4094 | 0.01 |
| energy-hotel-frame43frame50 | -4563 | 0.1 | -4563 | 0.01 |
| energy-hotel-frame43frame57 | -4532 | 0.2 | -4532 | 0.01 |

Continued on next page

Table 5 Continued from previous page

| | LB \uparrow | LB time [s] | UB \downarrow | UB time [s] |
|-----------------------------|---------------|-------------|-----------------|-------------|
| energy-hotel-frame43frame64 | -4450 | 0.2 | -4450 | 0.01 |
| energy-hotel-frame43frame71 | -4422 | 0.2 | -4422 | 0.01 |
| energy-hotel-frame43frame78 | -4351 | 0.2 | -4351 | 0.01 |
| energy-hotel-frame43frame85 | -4295 | 0.2 | -4295 | 0.01 |
| energy-hotel-frame43frame92 | -4221 | 0.2 | -4221 | 0.01 |
| energy-hotel-frame43frame99 | -4190 | 0.2 | -4190 | 0.01 |
| energy-hotel-frame50frame57 | -4566 | 0.1 | -4566 | 0.01 |
| energy-hotel-frame50frame64 | -4517 | 0.2 | -4517 | 0.01 |
| energy-hotel-frame50frame71 | -4463 | 0.1 | -4463 | 0.01 |
| energy-hotel-frame50frame78 | -4400 | 0.2 | -4400 | 0.01 |
| energy-hotel-frame50frame85 | -4342 | 0.2 | -4342 | 0.01 |
| energy-hotel-frame50frame92 | -4260 | 0.2 | -4260 | 0.01 |
| energy-hotel-frame50frame99 | -4240 | 0.2 | -4240 | 0.01 |
| energy-hotel-frame57frame64 | -4567 | 0.2 | -4567 | 0.01 |
| energy-hotel-frame57frame71 | -4508 | 0.2 | -4508 | 0.01 |
| energy-hotel-frame57frame78 | -4475 | 0.2 | -4475 | 0.01 |
| energy-hotel-frame57frame85 | -4398 | 0.2 | -4398 | 0.01 |
| energy-hotel-frame57frame92 | -4344 | 0.2 | -4344 | 0.01 |
| energy-hotel-frame57frame99 | -4332 | 0.2 | -4332 | 0.01 |
| energy-hotel-frame64frame71 | -4578 | 0.1 | -4578 | 0.01 |
| energy-hotel-frame64frame78 | -4545 | 0.2 | -4545 | 0.01 |
| energy-hotel-frame64frame85 | -4481 | 0.1 | -4481 | 0.01 |
| energy-hotel-frame64frame92 | -4413 | 0.2 | -4413 | 0.01 |
| energy-hotel-frame64frame99 | -4385 | 0.2 | -4385 | 0.01 |
| energy-hotel-frame71frame78 | -4550 | 0.2 | -4550 | 0.01 |
| energy-hotel-frame71frame85 | -4552 | 0.2 | -4552 | 0.01 |
| energy-hotel-frame71frame92 | -4469 | 0.1 | -4469 | 0.01 |
| energy-hotel-frame71frame99 | -4413 | 0.2 | -4413 | 0.01 |
| energy-hotel-frame78frame85 | -4589 | 0.1 | -4589 | 0.01 |
| energy-hotel-frame78frame92 | -4545 | 0.1 | -4545 | 0.01 |
| energy-hotel-frame78frame99 | -4534 | 0.2 | -4534 | 0.01 |
| energy-hotel-frame85frame92 | -4578 | 0.1 | -4578 | 0.01 |
| energy-hotel-frame85frame99 | -4528 | 0.1 | -4528 | 0.01 |
| energy-hotel-frame8frame15 | -4572 | 0.2 | -4572 | 0.01 |
| energy-hotel-frame8frame22 | -4491 | 0.2 | -4491 | 0.01 |
| energy-hotel-frame8frame29 | -4424 | 0.2 | -4424 | 0.01 |
| energy-hotel-frame8frame36 | -4379 | 0.2 | -4379 | 0.01 |
| energy-hotel-frame8frame43 | -4262 | 0.2 | -4262 | 0.01 |
| energy-hotel-frame8frame50 | -4179 | 0.2 | -4179 | 0.01 |
| energy-hotel-frame8frame57 | -4131 | 0.2 | -4131 | 0.01 |
| energy-hotel-frame8frame64 | -4060 | 0.2 | -4060 | 0.01 |
| energy-hotel-frame8frame71 | -4021 | 0.2 | -4021 | 0.01 |
| energy-hotel-frame8frame78 | -3931 | 0.2 | -3931 | 0.01 |
| energy-hotel-frame8frame85 | -3877 | 0.2 | -3877 | 0.01 |
| energy-hotel-frame8frame92 | -3802 | 0.3 | -3802 | 0.01 |
| energy-hotel-frame8frame99 | -3762 | 0.3 | -3762 | 0.02 |
| energy-hotel-frame92frame99 | -4593 | 0.1 | -4593 | 0.01 |

Table 6. Detailed results of FastDOG on *Graph matching - house* dataset

| | LB \uparrow | LB time [s] | UB \downarrow | UB time [s] |
|------------------------------|---------------|-------------|-----------------|-------------|
| MEAN | -3778 | 0.4 | -3778 | 0.01 |
| energy-house-frame10frame100 | -3720 | 0.6 | -3720 | 0.01 |
| energy-house-frame10frame95 | -3809 | 0.4 | -3809 | 0.01 |
| energy-house-frame10frame96 | -3786 | 0.4 | -3786 | 0.01 |
| energy-house-frame10frame97 | -3748 | 0.4 | -3748 | 0.01 |
| energy-house-frame10frame98 | -3766 | 0.4 | -3766 | 0.01 |
| energy-house-frame10frame99 | -3728 | 0.5 | -3728 | 0.01 |
| energy-house-frame11frame100 | -3739 | 0.5 | -3739 | 0.01 |
| energy-house-frame11frame101 | -3748 | 0.4 | -3748 | 0.01 |
| energy-house-frame11frame96 | -3809 | 0.4 | -3809 | 0.01 |
| energy-house-frame11frame97 | -3748 | 0.4 | -3748 | 0.01 |
| energy-house-frame11frame98 | -3781 | 0.4 | -3781 | 0.01 |
| energy-house-frame11frame99 | -3736 | 0.4 | -3736 | 0.02 |
| energy-house-frame12frame100 | -3768 | 0.5 | -3768 | 0.01 |
| energy-house-frame12frame101 | -3775 | 0.5 | -3775 | 0.01 |
| energy-house-frame12frame102 | -3783 | 0.5 | -3783 | 0.01 |
| energy-house-frame12frame97 | -3780 | 0.5 | -3780 | 0.01 |
| energy-house-frame12frame98 | -3807 | 0.5 | -3807 | 0.01 |
| energy-house-frame12frame99 | -3766 | 0.5 | -3766 | 0.01 |
| energy-house-frame13frame100 | -3749 | 0.5 | -3749 | 0.01 |
| energy-house-frame13frame101 | -3773 | 0.4 | -3773 | 0.01 |
| energy-house-frame13frame102 | -3775 | 0.4 | -3775 | 0.01 |
| energy-house-frame13frame103 | -3749 | 0.4 | -3749 | 0.01 |
| energy-house-frame13frame98 | -3798 | 0.4 | -3798 | 0.01 |
| energy-house-frame13frame99 | -3754 | 0.4 | -3754 | 0.01 |
| energy-house-frame14frame100 | -3785 | 0.5 | -3785 | 0.01 |
| energy-house-frame14frame101 | -3796 | 0.4 | -3796 | 0.01 |
| energy-house-frame14frame102 | -3806 | 0.4 | -3806 | 0.01 |
| energy-house-frame14frame103 | -3769 | 0.4 | -3769 | 0.01 |
| energy-house-frame14frame104 | -3761 | 0.5 | -3761 | 0.01 |
| energy-house-frame14frame99 | -3788 | 0.4 | -3788 | 0.01 |
| energy-house-frame15frame100 | -3784 | 0.5 | -3784 | 0.01 |
| energy-house-frame15frame101 | -3796 | 0.4 | -3796 | 0.01 |
| energy-house-frame15frame102 | -3798 | 0.4 | -3798 | 0.01 |
| energy-house-frame15frame103 | -3774 | 0.4 | -3774 | 0.01 |
| energy-house-frame15frame104 | -3762 | 0.4 | -3762 | 0.01 |
| energy-house-frame15frame105 | -3745 | 0.5 | -3745 | 0.01 |
| energy-house-frame16frame101 | -3804 | 0.4 | -3804 | 0.01 |
| energy-house-frame16frame102 | -3815 | 0.4 | -3815 | 0.01 |
| energy-house-frame16frame103 | -3787 | 0.3 | -3787 | 0.01 |
| energy-house-frame16frame104 | -3774 | 0.4 | -3774 | 0.01 |
| energy-house-frame16frame105 | -3752 | 0.4 | -3752 | 0.01 |
| energy-house-frame17frame102 | -3820 | 0.3 | -3820 | 0.01 |
| energy-house-frame17frame103 | -3799 | 0.3 | -3799 | 0.01 |
| energy-house-frame17frame104 | -3774 | 0.4 | -3774 | 0.01 |
| energy-house-frame17frame105 | -3756 | 0.4 | -3756 | 0.01 |
| energy-house-frame18frame103 | -3821 | 0.4 | -3821 | 0.01 |
| energy-house-frame18frame104 | -3794 | 0.4 | -3794 | 0.01 |

Continued on next page

Table 6 Continued from previous page

| | LB ↑ | LB time [s] | UB ↓ | UB time [s] |
|------------------------------|-------|-------------|-------|-------------|
| energy-house-frame18frame105 | -3777 | 0.4 | -3777 | 0.01 |
| energy-house-frame19frame104 | -3799 | 0.4 | -3799 | 0.01 |
| energy-house-frame19frame105 | -3767 | 0.4 | -3767 | 0.01 |
| energy-house-frame1frame86 | -3833 | 0.3 | -3833 | 0.01 |
| energy-house-frame1frame87 | -3808 | 0.3 | -3808 | 0.01 |
| energy-house-frame1frame88 | -3758 | 0.3 | -3758 | 0.01 |
| energy-house-frame1frame89 | -3776 | 0.4 | -3776 | 0.01 |
| energy-house-frame1frame90 | -3710 | 0.4 | -3710 | 0.01 |
| energy-house-frame1frame91 | -3761 | 0.4 | -3761 | 0.01 |
| energy-house-frame20frame105 | -3772 | 0.4 | -3772 | 0.01 |
| energy-house-frame2frame87 | -3837 | 0.3 | -3837 | 0.01 |
| energy-house-frame2frame88 | -3807 | 0.3 | -3807 | 0.01 |
| energy-house-frame2frame89 | -3807 | 0.3 | -3807 | 0.01 |
| energy-house-frame2frame90 | -3766 | 0.4 | -3766 | 0.01 |
| energy-house-frame2frame91 | -3791 | 0.4 | -3791 | 0.01 |
| energy-house-frame2frame92 | -3753 | 0.4 | -3753 | 0.01 |
| energy-house-frame3frame88 | -3808 | 0.4 | -3808 | 0.01 |
| energy-house-frame3frame89 | -3815 | 0.4 | -3815 | 0.01 |
| energy-house-frame3frame90 | -3761 | 0.4 | -3761 | 0.01 |
| energy-house-frame3frame91 | -3808 | 0.4 | -3808 | 0.01 |
| energy-house-frame3frame92 | -3769 | 0.5 | -3769 | 0.01 |
| energy-house-frame3frame93 | -3763 | 0.5 | -3763 | 0.01 |
| energy-house-frame4frame89 | -3826 | 0.4 | -3826 | 0.01 |
| energy-house-frame4frame90 | -3772 | 0.4 | -3772 | 0.01 |
| energy-house-frame4frame91 | -3813 | 0.4 | -3813 | 0.01 |
| energy-house-frame4frame92 | -3769 | 0.5 | -3769 | 0.01 |
| energy-house-frame4frame93 | -3770 | 0.5 | -3770 | 0.01 |
| energy-house-frame4frame94 | -3781 | 0.4 | -3781 | 0.01 |
| energy-house-frame5frame90 | -3757 | 0.4 | -3757 | 0.01 |
| energy-house-frame5frame91 | -3801 | 0.4 | -3801 | 0.01 |
| energy-house-frame5frame92 | -3759 | 0.4 | -3759 | 0.01 |
| energy-house-frame5frame93 | -3764 | 0.4 | -3764 | 0.01 |
| energy-house-frame5frame94 | -3765 | 0.4 | -3765 | 0.01 |
| energy-house-frame5frame95 | -3773 | 0.4 | -3773 | 0.01 |
| energy-house-frame6frame91 | -3824 | 0.4 | -3824 | 0.01 |
| energy-house-frame6frame92 | -3779 | 0.4 | -3779 | 0.01 |
| energy-house-frame6frame93 | -3780 | 0.4 | -3780 | 0.01 |
| energy-house-frame6frame94 | -3787 | 0.4 | -3787 | 0.01 |
| energy-house-frame6frame95 | -3794 | 0.5 | -3794 | 0.01 |
| energy-house-frame6frame96 | -3770 | 0.5 | -3770 | 0.01 |
| energy-house-frame7frame92 | -3764 | 0.5 | -3764 | 0.01 |
| energy-house-frame7frame93 | -3768 | 0.4 | -3768 | 0.01 |
| energy-house-frame7frame94 | -3771 | 0.4 | -3771 | 0.01 |
| energy-house-frame7frame95 | -3780 | 0.5 | -3780 | 0.01 |
| energy-house-frame7frame96 | -3755 | 0.5 | -3755 | 0.01 |
| energy-house-frame7frame97 | -3712 | 0.5 | -3712 | 0.01 |
| energy-house-frame8frame93 | -3787 | 0.5 | -3787 | 0.01 |
| energy-house-frame8frame94 | -3794 | 0.5 | -3794 | 0.01 |
| energy-house-frame8frame95 | -3800 | 0.5 | -3800 | 0.01 |

Continued on next page

Table 6 Continued from previous page

| | LB \uparrow | LB time [s] | UB \downarrow | UB time [s] |
|----------------------------|---------------|-------------|-----------------|-------------|
| energy-house-frame8frame96 | -3781 | 0.5 | -3781 | 0.01 |
| energy-house-frame8frame97 | -3738 | 0.5 | -3738 | 0.01 |
| energy-house-frame8frame98 | -3759 | 0.6 | -3759 | 0.01 |
| energy-house-frame9frame94 | -3806 | 0.3 | -3806 | 0.01 |
| energy-house-frame9frame95 | -3811 | 0.4 | -3811 | 0.01 |
| energy-house-frame9frame96 | -3797 | 0.4 | -3797 | 0.01 |
| energy-house-frame9frame97 | -3748 | 0.4 | -3748 | 0.01 |
| energy-house-frame9frame98 | -3770 | 0.5 | -3770 | 0.01 |
| energy-house-frame9frame99 | -3726 | 0.5 | -3726 | 0.01 |

Table 7. Detailed results of FastDOG on *Graph matching - worms* dataset

| | LB \uparrow | LB time [s] | UB \downarrow | UB time [s] |
|----------------------|---------------|-------------|-----------------|-------------|
| MEAN | -48934 | 51.4 | -48316 | 2.36 |
| worm01-16-03-11-1745 | -46447 | 38.2 | -46209 | 5.98 |
| worm02-16-03-11-1745 | -50003 | 24.6 | -49994 | 0.14 |
| worm03-16-03-11-1745 | -50566 | 26.5 | -50525 | 0.96 |
| worm04-16-03-11-1745 | -49372 | 59.2 | -48973 | 1.95 |
| worm05-16-03-11-1745 | -49914 | 40.6 | -49224 | 2.83 |
| worm06-16-03-11-1745 | -50497 | 35.8 | -50442 | 1.83 |
| worm07-16-03-11-1745 | -49748 | 50.5 | -46552 | 5.36 |
| worm08-16-03-11-1745 | -49517 | 38.2 | -49131 | 2.58 |
| worm09-16-03-11-1745 | -45431 | 176.3 | -44986 | 1.85 |
| worm10-16-03-11-1745 | -46972 | 103 | -41550 | 7.14 |
| worm11-16-03-11-1745 | -48868 | 76.1 | -48582 | 0.86 |
| worm12-16-03-11-1745 | -51032 | 49.9 | -50191 | 3.19 |
| worm13-16-03-11-1745 | -46243 | 66.6 | -45661 | 2.44 |
| worm14-16-03-11-1745 | -47636 | 39.4 | -46479 | 4.3 |
| worm15-16-03-11-1745 | -49573 | 35.6 | -49540 | 0.25 |
| worm16-16-03-11-1745 | -48948 | 39.1 | -48277 | 2.49 |
| worm17-16-03-11-1745 | -48175 | 48.2 | -48003 | 2.72 |
| worm18-16-03-11-1745 | -48390 | 24 | -48201 | 2.76 |
| worm19-16-03-11-1745 | -48966 | 44.1 | -48694 | 1.47 |
| worm20-16-03-11-1745 | -49536 | 38 | -49353 | 2.63 |
| worm21-16-03-11-1745 | -49893 | 68.2 | -49801 | 1.4 |
| worm22-16-03-11-1745 | -48233 | 48 | -47888 | 2.59 |
| worm23-16-03-11-1745 | -50020 | 34.9 | -49955 | 1.94 |
| worm24-16-03-11-1745 | -49679 | 30.5 | -49233 | 1.61 |
| worm25-16-03-11-1745 | -47312 | 101.6 | -47138 | 1.3 |
| worm26-16-03-11-1745 | -47537 | 47.6 | -45603 | 5.14 |
| worm27-16-03-11-1745 | -50075 | 41.2 | -50042 | 0.33 |
| worm28-16-03-11-1745 | -49516 | 25.5 | -49470 | 0.8 |
| worm29-16-03-11-1745 | -50110 | 66.1 | -50052 | 0.81 |
| worm30-16-03-11-1745 | -49804 | 24.3 | -49730 | 1.16 |

10.3. MRF

Table 8. Detailed results of FastDOG on *MRF - color-seg* dataset

| | LB \uparrow | LB time [s] | UB \downarrow | UB time [s] |
|----------------|---------------|-------------|-----------------|-------------|
| MEAN | 308472094 | 11.1 | 308474165 | 3.32 |
| colseg-cow3 | 455392703 | 12.6 | 455394996 | 4 |
| colseg-cow4 | 451816564 | 19.9 | 451820311 | 5.78 |
| colseg-garden4 | 18207016 | 0.9 | 18207187 | 0.17 |

Table 9. Detailed results of FastDOG on *MRF - color-seg-n4* dataset

| | LB \uparrow | LB time [s] | UB \downarrow | UB time [s] |
|--------------------------|---------------|-------------|-----------------|-------------|
| MEAN | 20011 | 8.5 | 20017 | 0.19 |
| clownfish-small | 14817 | 4.2 | 14818 | 0.26 |
| crops-small | 11923 | 5.5 | 11926 | 0.31 |
| fourcolors | 69520 | 0.5 | 69529 | 0.04 |
| lake-small | 14311 | 5.3 | 14313 | 0.19 |
| palm-small | 12236 | 17.6 | 12239 | 0.3 |
| penguin-small | 8234 | 7.3 | 8239 | 0.11 |
| pfau-small | 24231 | 21.5 | 24255 | 0.22 |
| snail | 13104 | 1 | 13105 | 0.04 |
| strawberry-glass-2-small | 11725 | 13.7 | 11728 | 0.23 |

Table 10. Detailed results of FastDOG on *MRF - color-seg-n8* dataset

| | LB \uparrow | LB time [s] | UB \downarrow | UB time [s] |
|--------------------------|---------------|-------------|-----------------|-------------|
| MEAN | 19990 | 13 | 19995 | 0.39 |
| clownfish-small | 14794 | 7.3 | 14795 | 0.41 |
| crops-small | 11853 | 9.4 | 11854 | 0.66 |
| fourcolors | 69550 | 0.7 | 69564 | 0.08 |
| lake-small | 14327 | 7.7 | 14329 | 0.31 |
| palm-small | 12253 | 26.7 | 12256 | 0.66 |
| penguin-small | 8258 | 11.8 | 8260 | 0.23 |
| pfau-small | 24008 | 31.9 | 24026 | 0.79 |
| snail | 13105 | 2.2 | 13106 | 0.09 |
| strawberry-glass-2-small | 11766 | 19.5 | 11768 | 0.32 |

Table 11. Detailed results of FastDOG on *MRF - object-seg* dataset

| | LB \uparrow | LB time [s] | UB \downarrow | UB time [s] |
|------------|---------------|-------------|-----------------|-------------|
| MEAN | 31317 | 45.3 | 31323 | 0.14 |
| objseg-349 | 2369 | 62.8 | 2386 | 0.21 |
| objseg-353 | 40634 | 103.5 | 40646 | 0.37 |
| objseg-358 | 38019 | 12.9 | 38019 | 0.01 |
| objseg-416 | 38160 | 20.7 | 38160 | 0.01 |
| objseg-552 | 37402 | 26.8 | 37402 | 0.1 |

10.4. QAPLib

Table 12. Detailed results of FastDOG on QAPLib - small dataset

| | LB \uparrow | LB time [s] | UB \downarrow | UB time [s] |
|--------|---------------|-------------|-----------------|-------------|
| MEAN | 3747352 | 89.4 | 43303812 | 48.53 |
| bur26a | 5313365 | 58.3 | 5710342 | 20.91 |
| bur26b | 3712826 | 59.3 | 4002866 | 22.82 |
| bur26c | 5314069 | 59.6 | 5886359 | 23.79 |
| bur26d | 3710949 | 59.7 | 4200747 | 25.05 |
| bur26e | 5313329 | 58.3 | 5839758 | 22.21 |
| bur26f | 3710993 | 59.9 | 4278500 | 24.92 |
| bur26g | 9977748 | 61.2 | 11109652 | 22.59 |
| bur26h | 6970285 | 59.8 | 7795328 | 24.23 |
| chr12a | 7916 | 21.7 | 12480 | 4.02 |
| chr12b | 6059 | 22.5 | 10162 | 4.55 |
| chr12c | 9791 | 22.2 | 12610 | 3.79 |
| chr15a | 7727 | 26.6 | 10606 | 4.56 |
| chr15b | 3759 | 26.4 | 11240 | 6.41 |
| chr15c | 8658 | 26.3 | 10282 | 2.8 |
| chr18a | 6637 | 29.8 | 14568 | 7.1 |
| chr18b | 1514 | 30.5 | 1814 | 2.46 |
| chr20a | 2155 | 30.7 | 4406 | 5.33 |
| chr20b | 2224 | 10.1 | 4576 | 5.38 |
| chr20c | 8319 | 33.6 | 28882 | 8.4 |
| chr22a | 5898 | 36.1 | 7116 | 5.84 |
| chr22b | 6071 | 31.5 | 6902 | 3.85 |
| chr25a | 3077 | 38.9 | 5290 | 6.31 |
| els19 | 9712306 | 37.3 | 23805836 | 14.55 |
| esc16a | 0 | 26.9 | 82 | 1.42 |
| esc16b | 0 | 28.4 | 310 | 2.43 |
| esc16c | 0 | 27.6 | 190 | 1.73 |
| esc16d | 0 | 27.5 | 24 | 0.63 |
| esc16e | 0 | 26.5 | 32 | 1.44 |
| esc16f | 0 | 25.9 | 0 | 0.01 |
| esc16g | 0 | 26.5 | 40 | 0.7 |
| esc16h | 299 | 30.3 | 1146 | 3.69 |
| esc16i | 0 | 26.6 | 22 | 0.41 |
| esc16j | 0 | 27.1 | 12 | 0.6 |
| esc32a | 0 | 56.2 | 368 | 4.55 |
| esc32b | 0 | 59.7 | 400 | 34.48 |
| esc32c | 0 | 60.8 | 850 | 10.38 |
| esc32d | 0 | 58.3 | 310 | 3.65 |
| esc32e | 0 | 48.3 | 2 | 0.19 |
| esc32f | 0 | 48.9 | 2 | 0.2 |
| esc32g | 0 | 47.4 | 8 | 1.03 |
| esc32h | 0 | 61.4 | 622 | 5.49 |
| had12 | 1368 | 21.8 | 1814 | 3.28 |
| had14 | 2027 | 24.1 | 3172 | 4.2 |
| had16 | 2468 | 29.8 | 3998 | 6.51 |
| had18 | 3425 | 34.5 | 5856 | 8.38 |

Continued on next page

Table 12 Continued from previous page

| | LB ↑ | LB time [s] | UB ↓ | UB time [s] |
|---------|----------|-------------|-----------|-------------|
| had20 | 4757 | 39.3 | 7634 | 10.15 |
| kra30a | 36471 | 88 | 144480 | 38.78 |
| kra30b | 36460 | 85.6 | 134300 | 37.48 |
| kra32 | 7281 | 63.5 | 24532 | 13.79 |
| lipa20a | 2840 | 39 | 3852 | 6.49 |
| lipa20b | 16950 | 37.8 | 34066 | 13.07 |
| lipa30a | 10401 | 86.8 | 13825 | 18.69 |
| lipa30b | 82583 | 82.5 | 196200 | 41.01 |
| lipa40a | 23604 | 267.7 | 32767 | 135.8 |
| lipa40b | 244077 | 264.2 | 621993 | 140.02 |
| lipa50a | 50567 | 523.8 | 64059 | 388.58 |
| lipa50b | 481647 | 514.1 | 1569702 | 437.65 |
| nug12 | 350 | 21.7 | 720 | 3.47 |
| nug14 | 540 | 25.2 | 1312 | 4.55 |
| nug15 | 598 | 27.5 | 1420 | 7.07 |
| nug16a | 768 | 29.7 | 2114 | 7.12 |
| nug16b | 655 | 29.5 | 1576 | 5.78 |
| nug17 | 826 | 31.4 | 2198 | 7.81 |
| nug18 | 903 | 34.5 | 2524 | 8 |
| nug20 | 1158 | 40.4 | 3118 | 9.73 |
| nug21 | 1034 | 42.7 | 3108 | 12.93 |
| nug22 | 1201 | 45.3 | 5322 | 15.3 |
| nug24 | 1448 | 51.6 | 4824 | 14.23 |
| nug25 | 1515 | 55.2 | 5022 | 18.59 |
| nug27 | 1873 | 56.4 | 7082 | 34.42 |
| nug28 | 1926 | 59.7 | 6836 | 35.77 |
| nug30 | 2239 | 85.6 | 8100 | 31.31 |
| rou12 | 136732 | 22.4 | 303114 | 7.16 |
| rou15 | 163890 | 28.3 | 436650 | 10.29 |
| rou20 | 279928 | 39.2 | 920170 | 17.66 |
| scr12 | 23784 | 21.7 | 41334 | 5.45 |
| scr15 | 39380 | 25.8 | 79850 | 7.76 |
| scr20 | 73910 | 35 | 188508 | 11.9 |
| sko42 | 4665 | 312.7 | 20198 | 163.27 |
| sko49 | 6254 | 497.2 | 29036 | 403.01 |
| ste36a | 5261 | 202.8 | 25616 | 98.78 |
| ste36b | 5261 | 200.2 | 100400 | 97.95 |
| ste36c | 5263021 | 200.2 | 19722744 | 125.68 |
| tai10a | 71410 | 19.3 | 162712 | 6.37 |
| tai10b | 971188 | 19.3 | 1235947 | 4.41 |
| tai12a | 120215 | 21.9 | 306868 | 7.37 |
| tai12b | 13788115 | 21.9 | 56755459 | 7.95 |
| tai15a | 154314 | 27.3 | 472096 | 10.77 |
| tai15b | 51183141 | 27.6 | 52878241 | 4.94 |
| tai17a | 184366 | 32 | 598290 | 13.21 |
| tai20a | 170523 | 39 | 889832 | 17.48 |
| tai20b | 24686130 | 40.1 | 195231805 | 21.36 |
| tai25a | 326908 | 56.4 | 1455224 | 27.28 |
| tai25b | 73310534 | 56.2 | 548164198 | 29.84 |

Continued on next page

Table 12 Continued from previous page

| | LB \uparrow | LB time [s] | UB \downarrow | UB time [s] |
|--------|---------------|-------------|-----------------|-------------|
| tai30a | 440217 | 85.8 | 2197658 | 44.54 |
| tai30b | 48043384 | 85.6 | 1295280184 | 60.82 |
| tai35a | 425910 | 181.3 | 2947642 | 99.65 |
| tai35b | 31126323 | 185.1 | 504198900 | 135.18 |
| tai40a | 511712 | 266.8 | 3735636 | 148.4 |
| tai40b | 51867467 | 267.9 | 1016709833 | 210.71 |
| tai50a | 694972 | 518.8 | 5929038 | 373.43 |
| tai50b | 34412453 | 528.3 | 759613745 | 429.98 |
| tho30 | 50192 | 82.8 | 193392 | 39.02 |
| tho40 | 79120 | 264 | 328136 | 144.48 |
| wil50 | 11341 | 523.5 | 55572 | 444.26 |

Table 13. Detailed results of FastDOG on *QAPLib* - large dataset

| | LB \uparrow | LB time [s] | UB \downarrow | UB time [s] |
|---------|---------------|-------------|-----------------|-------------|
| MEAN | 8924162 | 2713.6 | 137566865 | 4215.28 |
| esc128 | 0 | 373.9 | 192 | 9.79 |
| esc64a | 0 | 121.9 | 224 | 3.91 |
| lipa60a | 85472 | 1203.7 | 110137 | 836.39 |
| lipa60b | 946111 | 1197.5 | 3262713 | 814.44 |
| lipa70a | 130413 | 2142.2 | 173573 | 1597.51 |
| lipa70b | 1673026 | 3539 | 6000823 | 3408 |
| lipa80a | 215340 | 3545 | 258341 | 2823.49 |
| lipa80b | 2242309 | 5967.7 | 10172855 | 6052 |
| lipa90a | 245528 | 3547 | 367338 | 4727.65 |
| lipa90b | 3828710 | 3547.3 | 16340078 | 4932.2 |
| sko100a | 26946 | 3514.4 | 177118 | 8309.74 |
| sko100b | 27213 | 3511.4 | 180416 | 8423.26 |
| sko100c | 26378 | 3514.8 | 173824 | 8265.25 |
| sko100d | 26524 | 3514.9 | 175804 | 8618.05 |
| sko100e | 26619 | 3514.6 | 176208 | 8642.08 |
| sko100f | 26315 | 3515.1 | 173978 | 8693.04 |
| sko56 | 8628 | 968.2 | 41544 | 631.11 |
| sko64 | 11139 | 1569.9 | 58882 | 1156.87 |
| sko72 | 14205 | 2478.6 | 79146 | 1894.4 |
| sko81 | 18262 | 3561.4 | 108628 | 3111.76 |
| sko90 | 21746 | 3541.3 | 137230 | 5076.87 |
| tai100a | 1412256 | 3507.9 | 23975244 | 7753.14 |
| tai100b | 132097785 | 3514.7 | 1746517724 | 7731.76 |
| tai60a | 1230709 | 1209.9 | 8410894 | 774.26 |
| tai60b | 42883035 | 1240.6 | 997899804 | 819.49 |
| tai64c | 488264 | 186.7 | 2212584 | 39.62 |
| tai80a | 1242459 | 3563.6 | 15733802 | 2964.97 |
| tai80b | 69799747 | 3563.6 | 1156222051 | 3622.35 |
| wil100 | 45565 | 3516.5 | 297916 | 10509.61 |